




Characterization of nutrient status of *Halamphora luciae* (Bacillariophyceae) using matrix-assisted ultraviolet laser-desorption ionization time-of-flight mass spectrometry (MALDI-TOF MS)

Yasmin Daglio, María Laura Salum, María Cecilia Rodríguez, Rosa Erra-Balsells & María Cristina Matulewicz

To cite this article: Yasmin Daglio, María Laura Salum, María Cecilia Rodríguez, Rosa Erra-Balsells & María Cristina Matulewicz (2018): Characterization of nutrient status of *Halamphora luciae* (Bacillariophyceae) using matrix-assisted ultraviolet laser-desorption ionization time-of-flight mass spectrometry (MALDI-TOF MS), European Journal of Phycology, DOI: [10.1080/09670262.2018.1458336](https://doi.org/10.1080/09670262.2018.1458336)

To link to this article: <https://doi.org/10.1080/09670262.2018.1458336>

 View supplementary material 

 Published online: 10 Jul 2018.

 Submit your article to this journal 

 View Crossmark data 

Characterization of nutrient status of *Halamphora luciae* (Bacillariophyceae) using matrix-assisted ultraviolet laser-desorption ionization time-of-flight mass spectrometry (MALDI-TOF MS)

Yasmin Daglio^a, María Laura Salum^{a,b}, María Cecilia Rodríguez^c, Rosa Erra-Balsells^{a,b} and María Cristina Matulewicz^{a,b}

^aUniversidad de Buenos Aires, Consejo Nacional de Investigaciones Científicas y Técnicas. Centro de Investigación en Hidratos de Carbono (CIHIDECAR), Facultad de Ciencias Exactas y Naturales Pabellón II, 3er P., Ciudad Universitaria, 1428, Buenos Aires, Argentina; ^bUniversidad de Buenos Aires, Facultad de Ciencias Exactas y Naturales, Departamento de Química Orgánica, Pabellón II, 3er P., Ciudad Universitaria, 1428 Buenos Aires, Argentina; ^cUniversidad de Buenos Aires, Facultad de Ciencias Exactas y Naturales, Departamento de Biodiversidad y Biología Experimental, Ciudad Universitaria-Pabellón 2, C1428EGA Buenos Aires, Argentina

ABSTRACT

The effects of N and P depletion on the production and structural characterization of the cellular carbohydrate polymers of the estuarine diatom *Halamphora luciae* in batch culture were examined using matrix-assisted laser desorption-ionization time-of-flight mass spectrometry (MALDI-TOF MS) complemented with monosaccharide composition determination and structural analyses by methylation of aqueous extracted product. The MALDI MS analysis of the cells showed a similar profile in control and N- and P-depleted media, with a displacement to higher molecular weight for cells grown in depleted media. In the monosaccharide analyses, both nutrient depletion and culture ageing led to an increase in glucose content, indicating that MALDI-TOF MS in whole cells was detecting the changes in chrysolaminarin. The maxima for the ions from *f*/2-P and to a lesser extent in *f*/2-N were displaced to higher *m/z* values indicating a higher degree of polymerization (*DP*). Methylation analysis confirmed the presence of chrysolaminarin, a (1→3)-β-D-glucan with branching in C2 and C6, where the glucan backbone had a substitution every four glucose residues. The (1→3)-β-D-glucan was also detected in the cingule by fluorescence with aniline blue.

ARTICLE HISTORY Received 23 June 2017; Revised 11 January 2018; Accepted 8 February 2018

KEYWORDS Cellular carbohydrate polymers; chrysolaminarin; diatom cells; *Halamphora luciae*; MALDI-TOF MS; nutrient stress

Introduction

Widespread in oceans and continental aquatic bodies, in planktonic or benthic communities, diatoms are responsible for more than 40% of oceanic primary production (Nelson *et al.*, 1995; Field *et al.*, 1998; Armbrust, 2009; Tréguer *et al.*, 2017). Furthermore, diatoms are a key component of the biological carbon pump that exports carbon to the ocean interior, contributing significantly to the long-term sequestration of atmospheric CO₂ (Bowler *et al.*, 2010).

In rapidly growing cells, polysaccharides account for 10–50% of organic matter. They can be classified according to their location and function as cell-wall or storage polysaccharides (Granum *et al.*, 2002) or, based on the usual extraction methods, into water insoluble and soluble polymers. The former include structural polysaccharides associated with cell walls or frustules, such as mannans, glucuronomannans (Chiovitti *et al.*, 2003a; Le Costaouec *et al.*, 2017) and callose (Tesson & Hildebrand, 2013), and the latter comprise the storage polysaccharide

chrysolaminarin (Caballero *et al.*, 2016), exopolysaccharides and free sugars (Takahashi *et al.*, 2009).

Frustules are composed of silica and organic matter, including protein, long-chain polyamines and complex polysaccharides (Chiovitti *et al.*, 2003b; Le Costaouec *et al.*, 2017). Recently, a sulphated glucuronomannan with an important role in cell wall biogenesis was isolated from the frustules of *Phaeodactylon tricornutum* Bohlin (Le Costaouec *et al.*, 2017). Finally, the siliceous cell covering is enveloped by an external organic coat that is trapped within the secreted mucilaginous exopolysaccharide and/or glycoprotein during cell motion (Gügi *et al.*, 2015), usually termed extracellular polymeric substance.

The β-D-glucan chrysolaminarin, the main storage polysaccharide in diatoms, is located in vacuoles (Granum *et al.*, 2002). It consists of short chains of (1→3)-β-D-linked glucopyranosyl residues (*n* = 20–60) branched at C6 and/or C2 (McConville *et al.*, 1986; Alekseeva *et al.*, 2005; Storseth *et al.*, 2006). The average molecular weight and number of

branches of chrysolaminarin can vary significantly between species (Xia *et al.*, 2014). Chrysolaminarin contents of 12–33% DW (dry weight) have been documented in different diatom species (Mykkestad, 1989; Ju *et al.*, 2011). In culture, the content of chrysolaminarin is subject to diel variations (Caballero *et al.*, 2016) and has been reported either to increase (Mykkestad, 1989; Xia *et al.*, 2014; Hildebrand *et al.*, 2017) or to show little variation (Caballero *et al.*, 2016) with nutrient exhaustion and high irradiance. In diatom massive cultures, chrysolaminarin can be readily obtained as a water soluble product (Caballero *et al.*, 2016). It must be noted that the properties of β -glucans as immunostimulants and antioxidants have recently received attention (Barsanti *et al.*, 2011; Xia *et al.*, 2014).

From the point of view of biotechnological applications, inexpensive and rapid characterization of metabolites and/or optimal conditions to proceed with biomass harvest is highly desirable. Within this context, a method for obtaining fingerprint profiles, such as matrix-assisted ultraviolet laser-desorption ionization time-of-flight mass spectrometry (MALDI-TOF MS), is attractive. MALDI-TOF MS has been used in diatoms to characterize the polyamines and silaffin fractions (Sumper *et al.*, 2005, 2007; Sumper & Lehmann, 2006), lipids (Vieler *et al.*, 2007; Danielewicz *et al.*, 2011), chlorophylls (Suzuki *et al.*, 2009), and recently, to establish molecular mass fingerprinting profiles (Nicolau *et al.*, 2014) as well as the degree of polymerization of polysaccharides (Liang *et al.*, 2013; Ai *et al.*, 2015). Furthermore, MALDI-TOF MS is increasingly being applied in routine protocols for the reliable identification of bacteria (Ng, 2013; Sandrin *et al.*, 2013), fungi (Packer *et al.*, 2013; Pavlovic *et al.*, 2014) and microalgae (Nicolau *et al.*, 2014; Andrade *et al.*, 2015; Emami *et al.*, 2015) by referring to mass spectra in databases (Zhang *et al.*, 2015). It is claimed that MALDI-TOF MS-based fingerprint methods have greater taxonomic resolution than traditional molecular techniques (Giebel *et al.*, 2010; De Bruyne *et al.*, 2011) for economically relevant microorganisms (Knoshaug & Darzins, 2011; Smith & Crews, 2014).

Halamphora luciae (Cholnoky) Levkov is a cosmopolitan, brackish water species, present in the benthic biofilm community of the intertidal mudflat of Bahía Blanca Estuary, Argentina, that has recently been included in a screening of diatom species with potential biotechnological applications. At present, a strain of *Halamphora coffeaeformis* (C. Agardh) Levkov isolated from the same site is being assayed for the production of biodiesel (Martín *et al.*, 2016) with promising results. According to Hildebrand *et al.* (2017), triacylglycerol (TAG) accumulation in *Thalassiosira pseudonana* Hasle & Heimdal is correlated with a reduction in chrysolaminarin storage.

Therefore, we considered it interesting to follow the changes in the intracellular chrysolaminarin in *Halamphora luciae* by testing different culture media and harvesting points. This could provide clues for the choice of the end-point of the cultures and/or the culture conditions, depending on whether the cellular biomass would eventually be employed for the extraction of TAG or chrysolaminarin. The aim of the present research was to employ MALDI-TOF MS as a non-extractive method for attaining fingerprint profiles of cellular polysaccharides of *H. luciae* from different culture stages or under N and P starvation. MALDI-TOF spectra were complemented with monosaccharide composition and structural analyses by methylation of the water-soluble carbohydrate fraction extracted from the diatom cells to assess their identity.

Materials and methods

Algal cultures

Halamphora luciae cells were isolated from a mudflat located in Bahía Blanca Estuary (South Atlantic coast, 38°44'59.47"S, 62°22'51"W) by micropipetting. Unialgal axenic cultures were obtained as in Daglio *et al.* (2016). The strain has been maintained in our laboratory since 2013 in standard *f/2* medium (Guillard, 1975) and grown at 13°C in a 12:12 light-dark cycle using cool-white fluorescent light (100 $\mu\text{mol photons m}^{-2} \text{s}^{-1}$).

Experimental setting

To examine the effect of N and P on polysaccharides, cells were grown in sterilized seawater *f/2* medium (control), *f/2* without the addition of nitrate (*f/2-N*) and *f/2* without the addition of phosphate (*f/2-P*) for 15 days (Daglio *et al.*, 2016). To initiate the assays, exponentially growing cells in *f/2* were repeatedly washed and re-suspended in commercial seawater (30 psu) for pre-starvation for 2 days before inoculation in nutrient-depleted media.

For MALDI-TOF MS analysis of cells from different culture phases, harvest proceeded at days 5 (early exponential), 10 (late exponential), 15 (early stationary), 25 and 35 (late stationary) (Supplementary fig. S1).

Extraction of cell polysaccharides and structural analysis

Cellular polysaccharides were extracted from freeze-dried cells of *H. luciae* (4 g) with water at room temperature by magnetic stirring at 300 rpm for 30 min (product RTW). The supernatant was collected by centrifugation (10 000 $\times g$ for 30 min) and the

precipitate re-extracted with hot water at 100°C (product W100) for 1 h. The extracts were lyophilized and desalted with a Bio-Gel P-2 (Bio-Rad) column (RTW: yield, 0.460 g; W100: yield, 1.22 g).

For the structural analyses, RTW (42 mg) was methylated using powdered NaOH in dimethyl sulphoxide-iodomethane (Ciucanu & Kerek, 1984). The permethylated polysaccharide was extracted with chloroform (4 times) and the extracts dried off. The yield after the final methylation step (RTW-m) was 10.5 mg.

Monosaccharide composition

Sugar composition was determined by gas-liquid chromatography (GLC) after hydrolysis of the different products (i.e. whole cells from different culture conditions and products of extractions) with 2M trifluoroacetic acid (2 h at 121°C) followed by conversion of the monosaccharides to their alditol acetates (Albersheim *et al.*, 1967).

GLC of the alditol acetates and the partially methylated alditol acetates was carried out on a Hewlett-Packard 5890A gas-liquid chromatograph equipped with a flame ionization detector and fitted with a fused silica column (0.25 mm i.d. × 30 m) WCOT-coated with a 0.20 µm film of SP-2330. Chromatography was performed: (a) isothermally at 220°C for the alditol acetates; and (b) from 160°C to 210°C at 2°C min⁻¹, then from 210°C to 240°C at 5° min⁻¹ followed by a 30-min hold for partially methylated alditol acetates (Shea & Carpita, 1988). Nitrogen was employed as the carrier gas at a flow rate of 1 ml min⁻¹ with a split ratio 80:1. The injector and detector temperatures were set at 240°C. Assignments were referred to a mixture of standard alditol acetates. When necessary, GLC-MS analyses were carried out on a Shimadzu QP 5050 A (Kyoto, Japan) apparatus working at 70 eV using the same column and conditions described above, but using helium as a gas carrier at a total flow rate of 1 ml min⁻¹; the injector temperature was 240°C.

MALDI-TOF MS

Spectra were recorded on a BrukerUltraflex II TOF/TOF, controlled by the FlexControl 3.0 software (Bruker Daltonics, Bremen, Germany). Desorption/ionization was carried out using a frequency tripled Nd:YAG laser emitting at 355 nm with a 100 Hz shot frequency. All mass spectra were taken in the positive-linear and reflectron modes. Experiments were performed using first the full range setting for laser firing position in order to select the optimal position for data collection, and secondly fixing the laser firing position in the sample sweet spots. The laser power was adjusted to obtain high signal-to-noise ratio (S/

N) while ensuring minimal fragmentation of the parent ions and each mass spectrum was generated by averaging 500 laser pulses per spot. Spectra were obtained and analysed with the programs FlexControl and FlexAnalysis, respectively. MTP 384 target plate steel T F was used (Part No.: 209519; target frame (# 74115); 384 circular spots, 3.5 mm diameter; S/N 03630; Bruker, Bremen, Germany).

The following matrices were tested: 9H-pyrido[3,4b]indole (nor-harmane); α-cyano-4-hydroxycinnamic acid (CHCA); *E*-3,5-dimethoxy-4-hydroxycinnamic acid (sinapinic acid, SA) and 2,5 dihydroxybenzoic acid (DHBA). Mixtures of DHBA:CHCA (1:1; mol/mol) and DHBA:SA (1:1; mol/mol) in 1 ml of methanol:water (75:25, v/v) were also assayed. The stock solutions of the matrices were made by dissolving 10 mg of the selected matrix (or the mixture of matrices) in 1 ml of methanol (HPLC-grade)-H₂O (75:25, v/v). For external calibration β-cyclodextrin with nor-harmane as matrix were employed. All chemicals were purchased from Sigma-Aldrich.

For the MALDI-TOF MS analysis of the aqueous extracts (RTW and W100) two sample preparation methods were used. (a) Sandwich method or dry-droplet method (Nonami *et al.*, 1997): 0.5 µl of the matrix were transferred on a MALDI sample plate and dried at normal atmosphere. When the solvent was almost evaporated 0.5 µl of the aqueous extracts (10–20 mg ml⁻¹) were added on the matrix layer, dried at normal atmosphere and followed by further addition of 0.5 µl (× 2) of matrix solution (matrix-analyte ratio 3:1 (v/v)). (b) The experiments were also conducted using the mixture method. The analyte-matrix sample was prepared as a 1:1 (v/v) solution mixture and transferred (0.5 µl) on a MALDI sample plate and dried as described above.

For MALDI mass spectra of *H. luciae* entire cells, algal suspensions were concentrated by centrifugation at 500 × *g* for 3 min and 1 µl of diatom cell suspension was transferred on the MALDI sample plate, and dried at normal atmosphere before adding 1 µl of the matrix solution. All samples were dried at normal atmosphere and room temperature and analysed in duplicate and the measurement repeated on at least three different days. The degree of polymerization (*DP*) of the polymers was calculated based on the number of mass units (Ai *et al.*, 2015).

\bar{M}_n (number average molecular weight) and \bar{M}_w (weight average molecular weight) were calculated (Young & Lovell, 1991). The \bar{M}_n is the arithmetic mean of the molecular weight distribution of all the polymer chains in the sample, and is defined by the following equation:

$$\bar{M}_n = \frac{\sum N_i M_i}{\sum N_i}$$

where N_i is the number of chains of molecular weight M_i .

The \bar{M}_w , defined by the following equation, represents the contribution of the major polymer chain:

$$\bar{M}_w = \frac{\sum N_i M_i^2}{\sum N_i M_i}$$

Fluorescence microscopy

To detect (1→3)-β-D-glucan, early stationary cells (12 days) of *H. luciae* growing in *f/2* medium were incubated for 1 h in 0.05% aniline blue in 0.01M phosphate buffer, pH 8.5 (Krishnamurthy, 1999). Slides were examined under a Zeiss AxioScope microscope (Jena, Germany) equipped with UV (Ex 330–380 nm, FT 400 nm, Em 420 nm) and blue (Ex 450–490 nm, FT 510 nm, Em 520 nm) filter combinations and a digital photographic camera (Olympus C5000, Tokyo, Japan).

Statistical analyses

Statistical analyses were performed using InfoStat Release2014 (Di Rienzo *et al.*, 2014). One-way analysis of variance (ANOVA) was used to determine statistical significance and Tukey's honestly significant difference tests were used for post hoc treatment comparisons. The significance level was fixed at $P < 0.05$.

Results

Aqueous extracts RTW and W100 from cells in *f/2* medium

Room temperature aqueous extraction from cells in *f/2* medium yielded a product RTW whose monosaccharide composition, obtained after acid hydrolysis, indicated that glucose was the main component (Table 1). The product extracted with hot water (W100) showed an increase in the molar percentages of fucose and galactose and a decrease in glucose.

MALDI mass spectra of RTW and W100 extracts (Fig. 1, Table 2) were similar, showing unit intervals

Table 1. Monosaccharide composition (mol%) of the different extracts from *Halophora luciae* cells cultured in *f/2* medium. Data are expressed as media ± SD.

Monosaccharide ^a	RTW	W100
Rha	tr	3.7 ± 0.5
Fuc	8.5 ± 0.5	25.4 ± 2.1
Ara	2.9 ± 1.2	nd
Xyl	4.1 ± 0.9	3.2 ± 0.5
Man	5.9 ± 2.2	8.7 ± 2.4
Gal	13.9 ± 1.5	20.5 ± 0.6
Glc	64.7 ± 3.1	38.6 ± 0.3

^aRha=Rhamnose; Fuc=Fucose; Ara=arabinose; Xyl=Xylose; Man=Mannose; Gal=Galactose; Glc=Glucose; tr=trace (< 1 mol %); nd=not determined.

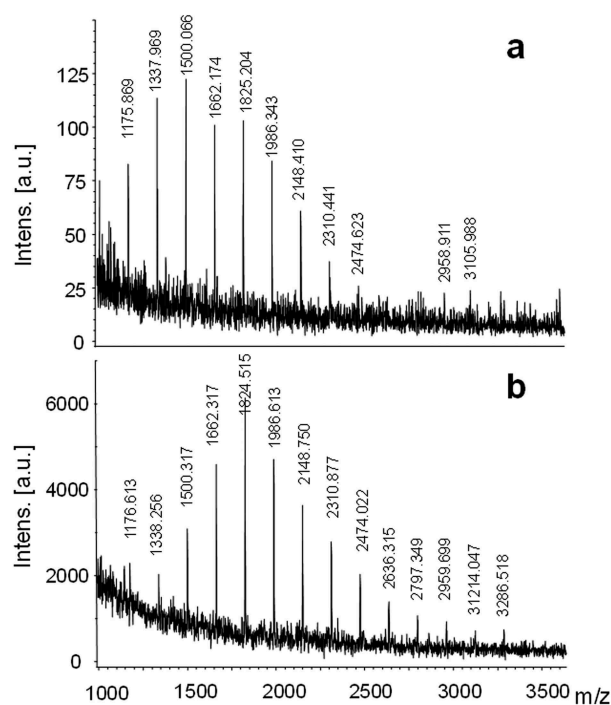


Fig. 1. MALDI mass spectra of the (a) room temperature (RTW) and (b) hot water (W 100) extraction from *Halophora luciae* cells grown in *f/2* medium. Matrix: DHBA-SA mixture.

Table 2. Average molecular weights obtained for MALDI mass spectrometry of *Halophora luciae* extracts in *f/2* medium.

	\bar{M}_n	\bar{M}_w	DP_{max}^a	DP_n^b	DP_{range}
RTW	1769	1893	9	13	7–19
W100	2255	2120	11	14	7–20

^a Degree of polymerization (DP) corresponding to the most abundant ion. ^b Number-average degree of polymerization calculated considering all the observed ions.

of m/z 162 in the molecular weight range, from m/z 1175.8 to 3105.9 for RTW and from m/z 1176.6 to 3286.5 for W100.

Methylation analysis of RTW indicated the presence of a (1→3)-linked glucan with branching at C2 and C6 (Table 3). The ratio of tetramethylated terminal glucose residues (20.8%) to the rest of the glucose

Table 3. Composition (mol %) of monosaccharide produced by methylation and hydrolysis of the RTW extract from *Halophora luciae*. Data are expressed as media ± SD.

Monosaccharide ^a	Deduced glycosidic linkage	RTW-m
2,3,4,6-Me ₄ Glc	Terminal	20.8 ± 1.4
2,4,6-Me ₃ Glc	3-linked	47.4 ± 3.9
4,6-Me ₂ Glc	3-linked	10.6 ± 1.7
2,4-Me ₂ Glc	2-substituted	12.7 ± 2.3
	3-linked	
Glc	6-substituted	8.5 ± 1.9

^a2,4-Me₂Glc=1,3,5,6-tetra-O-acetyl-2,4-di-O-methylglucitol; 4,6-Me₂Glc=1,2,3,5-tetra-O-acetyl-4,6-di-O-methylglucitol; 2,4,6-Me₃Glc=1,3,5-tri-O-acetyl-2,4,6-tri-O-methylglucitol; 2,3,4,6-Me₄Glc=1,5-di-O-acetyl-2,3,4,6-tetra-O-methylglucitol.

Table 4. Constituent monosaccharide (mol%) of extracts obtained from the hydrolysates of entire cells of *Halamphora luciae* cultured in *f/2*, *f/2-N* and *f/2-P* media. Data are expressed as media \pm SD.

Monosaccharide ^a	<i>f/2</i> _{10d} ^b	<i>f/2</i> _{20d} ^c	<i>f/2</i> _{30d} ^d	<i>f/2-N</i> ^e	<i>f/2-P</i> ^e
Rha	2.1 \pm 0.4	3.4 \pm 0.4	4.1 \pm 0.4	tr	2.1 \pm 1.4
Fuc	15.2 \pm 0.3	11.5 \pm 1.5	12.5 \pm 1.6	2.2 \pm 0.1	2.5 \pm 0.9
Ara	tr	nd	nd	tr	nd
Xyl	tr	1.9 \pm 1.2	nd	tr	17.5 \pm 2.3
Man	3.2 \pm 0.9	2.4 \pm 0.8	4.8 \pm 1.5	tr	8.9 \pm 4.1
Gal	34.6 \pm 1.1	21.5 \pm 0.4	16.1 \pm 0.1	2.9 \pm 0.9	6.2 \pm 0.5
Glc	43.9 \pm 0.8	58.9 \pm 0.9	62.5 \pm 0.5	94.9 \pm 0.3	62.8 \pm 1.3

^a Rha=Rhamnose; Fuc=Fucose; Ara=arabinose; Xyl=Xylose; Man=Mannose; Gal=Galactose; Glc=Glucose; tr=trace (< 1 mol %), nd=not determined. ^b Cells were grown in *f/2* medium and harvested at day 10. ^c Cells were grown in *f/2* medium and harvested at day 20. ^d Cells were grown in *f/2* medium and harvested at day 30. ^e Cells harvested at day 10.

units (79.2%) showed that the glucan backbone was substituted every four glucose residues.

Hydrolysis of entire cells

The entire cells were hydrolysed and the monosaccharide composition of the hydrolysates was determined (Table 4). At least *c.* 1.5–2 fold increase ($P < 0.05$) in glucose content was observed in P- and N-depleted media with respect to control in *f/2* in cells harvested at day 10. Control cells also exhibited high galactose and fucose molar percentages in contrast to cells in nutrient-depleted media. Xylose molar percentage was high in cells grown in P-depleted medium compared with the other two media. Nevertheless, hydrolysed cells grown in *f/2* over 20 and 30 days showed a significant increase ($P < 0.05$) in glucose molar percentage and a significant decline ($P < 0.05$) of galactose when compared with younger *f/2* cells (Table 4).

MALDI-TOF MS analysis of entire cells

Either in complete or in nutrient-deficient media, MALDI mass spectra of the entire cells harvested at day 15 exhibited unit intervals of m/z 162 (Fig. 2). Cells grown in *f/2* exhibited signals in the molecular weight range from m/z 4256.5–6363.9 (Fig. 2a). For cells from *f/2-N*, signals were detected in the molecular weight range located from m/z 2473.4–7011.4 (Fig. 2b), while for cells from *f/2-P* a molecular-weight range from m/z 4906.1–7660.2 was found (Fig. 2c). The \bar{M}_w and \bar{M}_n of the cell polysaccharides from *f/2* and N-depleted media were lower than those from P-depleted media (Table 5).

Representing the abundance relative to the most intense signal for each polymer (Fig. 3a), the maxima for the ions from *f/2-P* and to a lesser extent in *f/2-N* were displaced to higher m/z values indicating a higher *DP*. The polysaccharides from *f/2-N* and *f/2-P* gave a higher proportion of molecular weight oligomers with a *DP* range of 15–43 for the former and 27–47 for the latter (Fig. 3a, Table 5). It is worth noting that the proportion of low molecular weight

polysaccharide also increased in *f/2-N* compared with the control and *f/2-P* (Fig. 3a).

Since culture ageing is associated with nutrient depletion, we also analysed cells from *f/2* medium harvested at different times. MALDI analysis showed unit intervals of m/z 162 in all cases (Fig. 4). On day 5, two distributions of signals were detected, one corresponding to low molecular weight oligomers from m/z 2312.5–4420.7 and another incipient distribution with oligomers of higher molecular weight

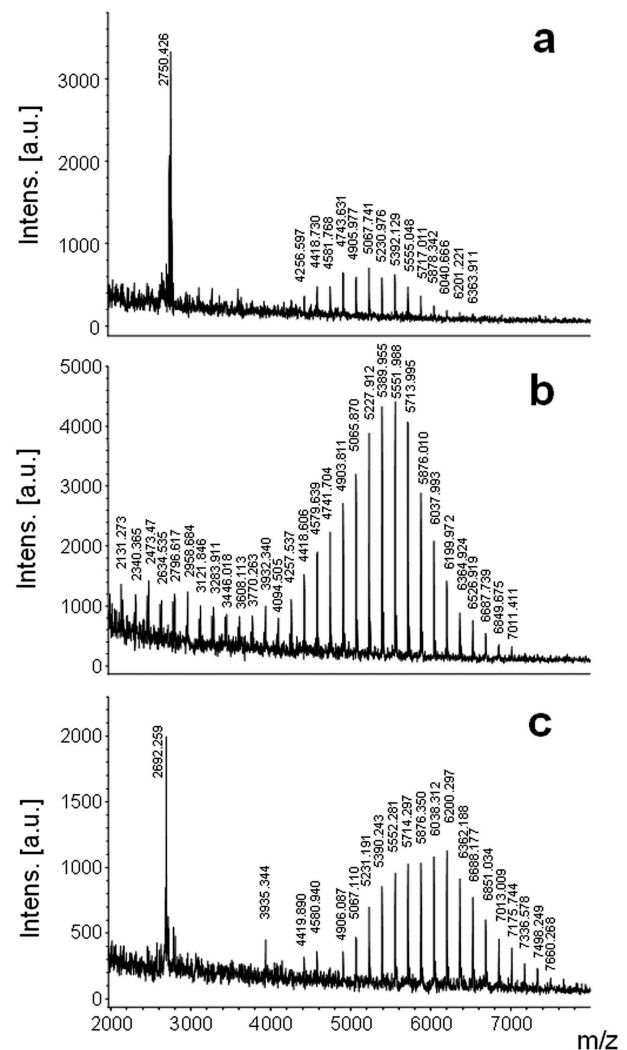


Fig. 2. MALDI mass spectra of *Halamphora luciae* cells under different culture media harvested at day 15. (a) *f/2* (control), (b) *f/2-N* and (c) *f/2-P*. Matrix: CHCA.

Table 5. Average molecular weights obtained for MALDI mass spectrometry of *Halamphora luciae* cells in different culture conditions and culture ages.

	\bar{M}_n	\bar{M}_w	DP_{max}^c	DP_n^d	DP_{range}
Growth medium^a					
<i>f</i> /2 medium	5192	5243	32	32	26–38
N depleted medium	4921	5062	34	30	15–43
P depleted medium	5983	6073	38	38	27–47
Culture age^b					
5-day culture	3936	4223	19	27	14–38
10-day culture	4666	4931	32	29	15–40
15-day culture	4703	5104	32	29	13–42
25-day culture	5187	5267	32	32	23–41
35-day culture	4973	5221	32	30	14–44

^a The cells of *H. luciae* harvested at day 15. ^b Cells were grown in *f*/2 medium. ^c Degree of polymerization (*DP*) corresponding to the most abundant ion. ^d Number-average degree of polymerization calculated considering all the observed ions.

from m/z 4582.7–6040.6 (Fig. 4a), with a higher relative intensity for the first group. At day 10, we observed the same two groups of signals, but in this case the higher signal intensity corresponded to the oligomers of higher molecular weight in the range of

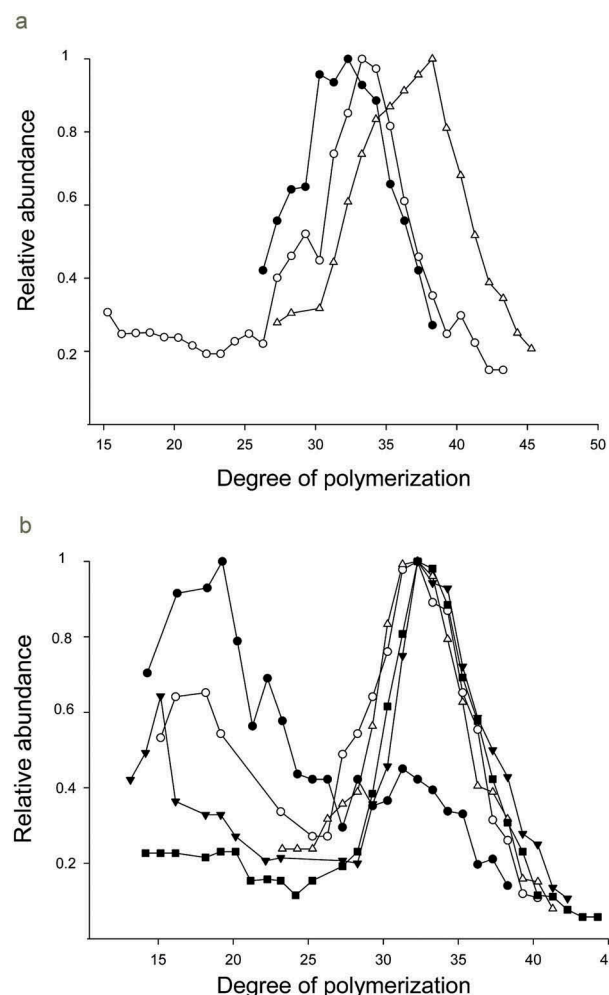


Fig. 3. (a) Distribution of the polymerization of the polymers from *Halamphora luciae* cells grown in *f*/2 medium (black circles), *f*/2-N (white circles) and *f*/2-P (white triangles), (b) Cells grown in *f*/2 medium and harvested at days 5 (black circles), 10 (white circles), 15 (black triangles), 25 (white triangles) and 35 (black squares). The relative abundance was based on the polymer with the most abundant ion, which was represented as one unit in the curve.

m/z 4094.4–6525.0 (Fig. 4b). Days 15 and 25 presented a dominant group of signals at high molecular weight (day 15: m/z 4419.8–6849.7; day 25: m/z 3769.4–6688.9) (Fig. 4c–d). At day 35, signals were detected in the molecular weight range m/z 2130.4–7175.9 (Fig. 4e). Table 5 shows the gradual displacement towards higher molecular weight ranges with time. This is clearly reflected in Fig. 3b, where the bimodality of the relative abundance of different *DP* fragments is gradually lost after day 15.

Cells from *f*/2 exhibited a continuous fluorescent strip in the cingule when stained with fluorochrome aniline blue (Figs 5–7). Additionally, fluorescent vacuoles could be detected in cells from control cultures.

Discussion

Aqueous extraction of the cells of *H. luciae* (especially at room temperature) rendered products with glucose as the major component. The presence of a (1→3)-linked glucan was proven by methylation analyses, suggesting, as pointed out by Chiovitti *et al.* (2004), that this glucan derives from chrysolaminarin. Differing from the report of Caballero *et al.* (2016), rising temperature did not improve glucose yield in the extract. This can be attributed to the fact that extraction at room temperature used lyophilized cells, where leakage of cellular components could be expected due to membrane rupture. As reported by Xia *et al.* (2014), glucose in RTW was accompanied by smaller molar percentages of galactose, fucose and mannose probably derived from extracellular polysaccharides with complex linkages and branching (Caballero *et al.*, 2016). The absence of these sugar moieties in the permethylated product could reflect the loss of soluble low molecular weight oligosaccharides during dialysis after methylation.

According to our structural analyses by methylation, chrysolaminarin in *H. luciae* has branching at C2 and C6 as reported for analogous polymers in *Stauroneis amphioxys* (McConville *et al.*, 1986), *Skeletonema costatum* (Paulsen & Myklestad, 1978), *Craspedostauros*

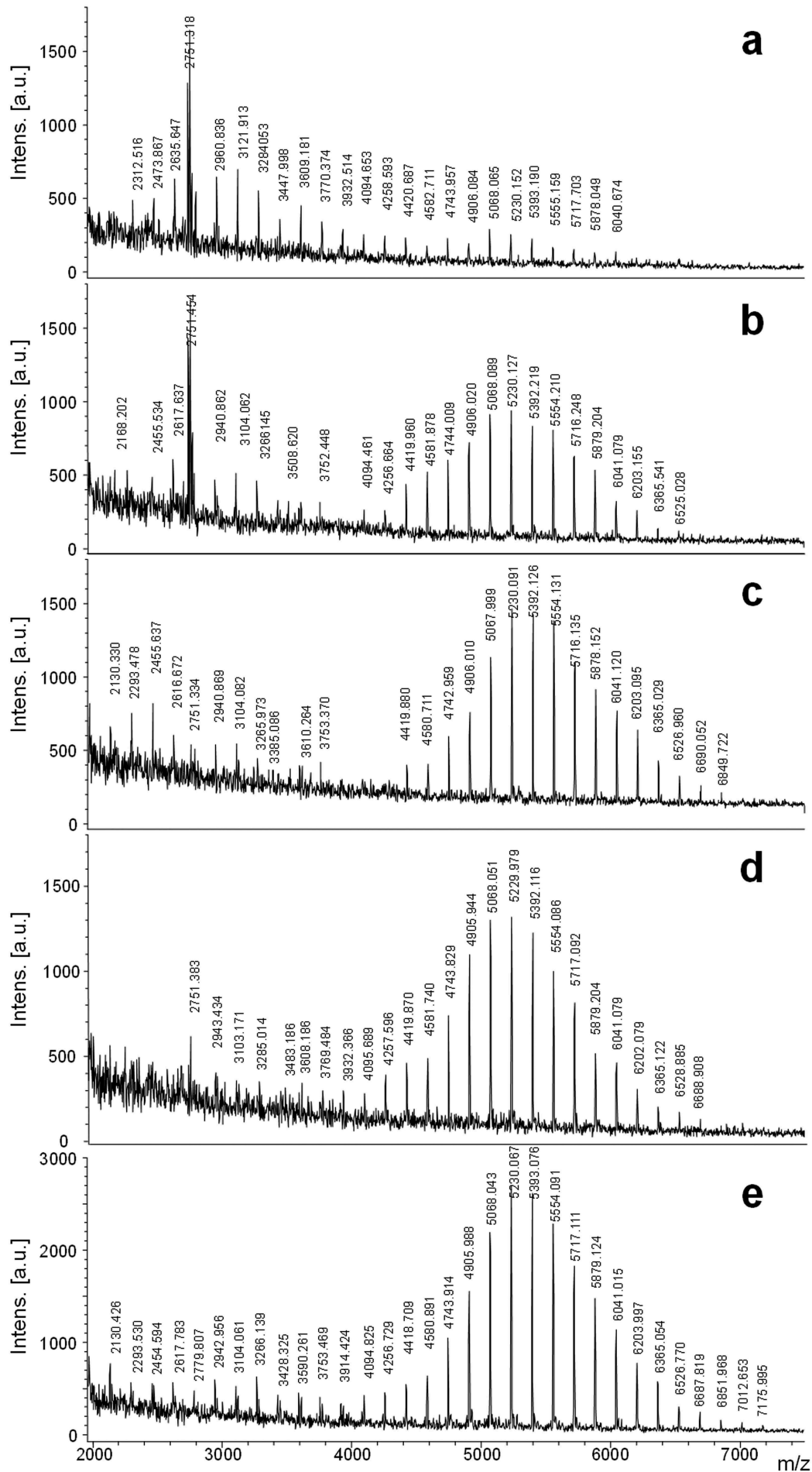
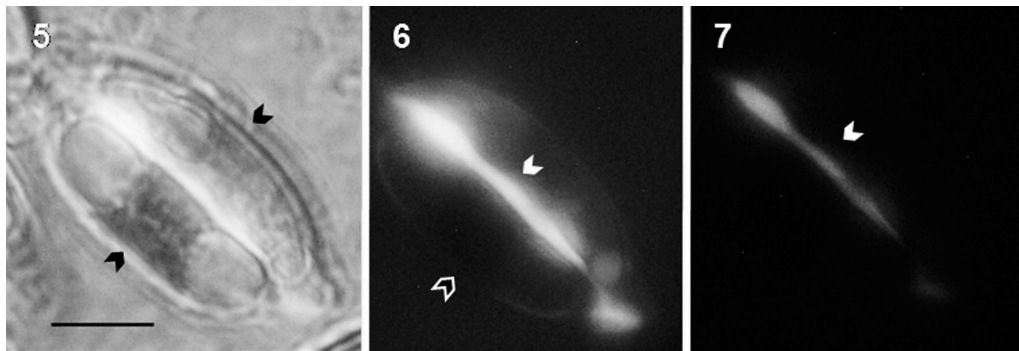


Fig. 4. MALDI mass spectra of *Halamphora luciae* cells growth in $f/2$ medium harvested at days (a) 5, (b) 10, (c) 15, (d) 25 and (e) 35. Matrix: SA.



Figs 5–7. *Halamphora luciae* cells cultured in *f/2* medium and stained with aniline blue. **Fig. 5.** Arrows in the light micrographs indicate the chloroplast. **Figs 6–7.** Fluorescence micrographs with (Fig. 6) blue filter (Ex 450–490 nm, 510 nm FT, and Em 520 nm) showing chlorophyll autofluorescence (black arrow) and (Fig. 7) with UV filter (Ex 330–380 nm, FT 400 nm, Em 420 nm) without chlorophyll autofluorescence. In Figs 6–7 the brighter fluorescence at the girdle bands indicates the presence of a β -1,3 glucan (white arrows). Scale = 10 μ m.

australis and *Thalassiosira pseudonana* (Chiovitti *et al.*, 2004). Whether substitution in C2 is missing or not, branching in C6 is always present, as reported for *Phaeodactylum tricorutum* (Beattie *et al.*, 1961; Chiovitti *et al.*, 2004; Caballero *et al.*, 2016), *Aulacoseira baicalensis* (Paulsen & Mykkestad, 1978), *Cylindrotheca fusiformis* (Chiovitti *et al.*, 2004), *Stephanodiscus meyerii* (Alekseeva *et al.*, 2005), *Chaetoceros debilis* (Storseth *et al.*, 2006) and *Odontella aurita* (Xia *et al.*, 2014). It is worth noting that the presence of β -(1→6)-linkages in chrysolaminarin is considered a prerequisite for immunostimulant activity (Kim *et al.*, 2011). For the storage glucan of *H. luciae* we estimated a *DB* (degree of branching) of 0.28. A wide range of *DB* from 0.015 to 0.39 has been reported (Beattie *et al.*, 1961; Paulsen & Mykkestad, 1978; Chiovitti *et al.*, 2004; Alekseeva *et al.*, 2005; Xia *et al.*, 2014; Caballero *et al.*, 2016). This is not surprising, since, according to our results, molecular weight can vary with culture nutritional state and/or age and this eventually may also modify the *DB*.

The presence of the structural polysaccharide callose cannot be ruled out, especially taking into account aniline blue fluorescence of the cingules. In fact, callose in frustules was reported previously (Waterkeyn & Bienfait, 1987). Only recently Tesson & Hildebrand (2013) assessed the role of callose in frustule integrity and/or silica deposition by employing inhibitors of (1→3)- β -glucan synthase. Yet, callose differs from chrysolaminarin as it is a non-branched glucan and poorly soluble in water (Stone, 2006).

The MALDI MS analysis of the cells showed a similar profile in the three culture media, with a displacement to higher molecular weight for the deprived media (Table 5). These changes in the MALDI-TOF MS profiles in the whole cells, both in nutrient-deprived media and in ageing cultures, reveal changes in polysaccharide molecular weight distribution. It should be kept in mind that

MALDI-TOF MS cannot account for differences in hexose identity in the polysaccharides. However, the increase in glucose content in the cell hydrolysates allows us to assume that the molecular weight distribution observed in MALDI profiles is mainly due to chrysolaminarin (Table 4). If we relate accumulation of the storage glucan with the displacement to increased relative abundance of higher *DP* signals, this effect was evident in aged and N- and P-deprived cultures of *H. luciae*. Moreover, *DP* was higher in nutrient-limited cultures than in complete *f/2* medium, especially in the absence of P. Accumulation of chrysolaminarin was reported for *Chaetoceros affinis*, *S. costatum* and *Thalassiosira fluviatilis* (Mykkestad, 1989) in stationary phase cultures. The diatom *Odontella aurita* (Xia *et al.*, 2014) showed a maximum of chrysolaminarin content in low N cultures. In *P. tricorutum*, Caballero *et al.* (2016), when following the diel variations in the chrysolaminarin pool under N starvation, concluded that there was no daily oscillation, suggesting no consumption in the dark to fuel heterotrophic metabolism in N-limited conditions (Jallet *et al.*, 2016). On the other hand, signals of smaller *DP* in the exponential and early stationary phase of *H. luciae* point to active biosynthesis of the storage glucan in earlier culture stages. As pointed out by Hildebrand *et al.* (2017) diatoms do not fully rely on storage carbohydrate for energy generation during cell division, so small molecular weight fragments observed in *H. luciae* would not derive from catabolism.

Under nutrient-replete, autotrophic conditions, high CO₂ assimilation by the Calvin cycle provides carbon skeletons for amino acid biosynthesis (especially during the dark period), fatty acid biosynthesis and mitochondrial TCA cycle for energy production (Brembu *et al.*, 2017). Diatoms allocate organic carbon to two primary storage metabolites: the neutral lipid triacylglycerol and the storage polysaccharide chrysolaminarin (Wilhelm *et al.*, 2006). Under nutrient

deficiency, particularly nitrogen starvation, diatoms accumulate TAGs (Abida *et al.*, 2015; Caballero *et al.*, 2016), which is of great interest in relation to biodiesel production (Hockin *et al.*, 2012; Obata *et al.*, 2013; Alipanah *et al.*, 2015; Levitan *et al.*, 2015; Barnech Bielsa *et al.*, 2016). Under P and N limitation, cell division eventually halts. Due to the reduced requirements of carbon skeletons for protein and phospholipid biosynthesis, more CO₂ is fixed through the Calvin cycle than is consumed. In order to deal with the excess carbon, carbon flow is instead directed toward storage as TAG, chrysolaminarin and excretion from the cell as extracellular polysaccharides (Daglio *et al.*, 2016; Brembu *et al.*, 2017). Recently, Hildebrand *et al.* (2017) demonstrated that under silicon starvation there was an upregulation in the direction of gluconeogenesis in both the cytoplasm and the chloroplast, consistent with the flux of carbon towards chrysolaminarin biosynthesis and accumulation.

Assaying with different matrices allowed us to reduce spectra baselines, a crucial feature in the distinction of different molecular weight fragments depending on age and/or culture conditions (especially those appearing with low intensity). The fingerprint obtained for *H. luciae* showed a bimodality which was not so evident in the spectra of the cells of the centric diatoms *T. pseudonana* or *Coscinodiscus* sp., which exhibited fragments in the *m/z* of 2000–6300 with unit intervals of 162 (Nicolau *et al.*, 2014; Ai *et al.*, 2015). It is noteworthy that the spectra of the pennate diatom *Seminavis robusta* showed great variability, which the authors attributed to the contribution of different strains and/or mating types in the samples analysed (Nicolau *et al.*, 2014).

In conclusion, chrysolaminarin can be used as an indicator of nutritional status by calibration of MALDI signatures for different species in order to select appropriate harvesting points in massive culture for the exploitation of this polysaccharide, with potential application as immunostimulants or food additives for farmed shrimp, fish, poultry and cattle.

Acknowledgements

The authors want to especially thank Dr Nora I. Maidana (DBBE, FCEN, UBA) for help in the identification of this diatom.

Disclosure statement

No potential conflict of interest was reported by the authors.

Funding

This work was funded by grants from UBA [GC 20020100100479, GC 20020130100216BA and 2002013010

0055BA] and CONICET [PIP 11220080100234, PIP 11220110100208 and PIP 0072CO] and ANPCyT [PICT 2012-0888]. The MALDI Ultraflex II (Bruker) TOF/TOF mass spectrometer was supported by a grant from ANPCYT, PME 125 (CEQUIBIEM, FCEN, UBA). YD is a Research Fellow of the National Research Council of Argentina (CONICET) and MLS, MCM and REB are research members of the same institution.

Author contributions

Y. Daglio: isolation of algae and growth tests, LM images, monosaccharide composition, data analysis and editing manuscript; M.L. Salum: MALDI mass spectrometry experiments, data analysis and editing manuscript; M.C. Rodríguez: growth experiments design, project direction, data analysis, drafting and editing manuscript; R. Erra-Balsells: MALDI spectra analysis and editing manuscript; M.C. Matulewicz: project direction, data analysis, drafting and editing manuscript.

Supplementary information

The following supplementary material is accessible via the Supplementary Content tab on the article's online page at <http://dx.doi.org/10.1080/09670262.2018.1458336>

Supplementary fig. S1: Growth curves of *Halimnobia luciae* in 100 ml beakers containing 40 ml of *f/2* (black square), *f/2-N* (white triangle) and *f/2-P* (white circle) media. Values represent the mean \pm *s* (*n* = 3).

References

- Abida, H., Dolch, L.J., Meï, C., Villanova, V., Conte, M., Block, M.A., Finazzi, G., Bastien, O., Tirichine, L., Bowler, C., Rébeillé, F., Petroustos, D., Jouhet, J. & Maréchal, E. (2015). Membrane glycerolipid remodeling triggered by nitrogen and phosphorus starvation in *Phaeodactylum tricorutum*. *Plant Physiology*, **167**: 118–136.
- Ai, X.X., Liang, J.R., Gao, Y.H., Lo, S.C.L., Lee, F.W.F., Chen, C.P., Luo, C.S. & Du, C. (2015). MALDI-TOF MS analysis of the extracellular polysaccharides released by the diatom *Thalassiosira pseudonana* under various nutrient conditions. *Journal of Applied Phycology*, **27**: 673–684.
- Albersheim, P., Nevins, D.J., English, P.D. & Karr, A. (1967). A method for the analysis of sugars in plant cell-wall polysaccharides by gas-liquid chromatography. *Carbohydrate Research*, **5**: 340–345.
- Alekseeva, S.A., Shevchenko, N.M., Kusaykin, M.I., Ponomorenko, L.P., Isakov, V.V., Zvyagintseva, T.N. & Likhoshvai, E.V. (2005). Polysaccharides of diatoms occurring in Lake Baikal. *Applied Biochemistry Microbiology*, **41**: 185–191.
- Alipanah, L., Rohloff, J., Winge, P., Bones, A.M. & Brembu, T. (2015). Whole-cell response to nitrogen deprivation in the diatom *Phaeodactylum tricorutum*. *Journal of Experimental Botany*, **66**: 6281–6296.
- Andrade, L.M., Mendes, M.A., Kowalski, P. & Nascimento, C.A.O. (2015). Comparative study of different matrix/solvent systems for the analysis of crude lyophilized microalgal preparations using matrix-assisted laser desorption/ionization time-of-flight mass spectrometry. *Rapid Communications in Mass Spectrometry*, **29**: 295–303.

- Armbrust, V. (2009). The life of diatoms in the world's oceans. *Nature*, **459**: 185–192.
- Barnech Bielsa, G., Popovich, C., Rodríguez, M.C., Martínez, A.M., Martín, L., Matulewicz, M.C. & Leonardi, P. (2016). Simultaneous production assessment of triacylglycerols for biodiesel and exopolysaccharides as valuable co-products in *Navicula cincta*. *Algal Research*, **15**: 120–128.
- Barsanti, L., Passarelli, V., Evangelista, V., Frassanito, A.M. & Gualtieri, P. (2011). Chemistry, physico-chemistry and applications linked to biological activities of β -glucans. *Natural Product Reports*, **28**: 457–466.
- Beattie, A., Hirst, E.L. & Percival, E. (1961). Studies on the metabolism of the Chrysophyceae. *Biochemical Journal*, **79**: 531–536.
- Bowler, C., Vardi, A. & Allen, A.E. (2010). Oceanographic and biogeochemical insights from diatom genomes. *Annual Review of Marine Science*, **2**: 333–365.
- Brembu, T., Mühlroth, A., Alipanah, L. & Bones, A.M. (2017). The effects of phosphorus limitation on carbon metabolism in diatoms. *Philosophical Transactions Royal Society B*, **372**: 20160406.
- Caballero, M.A., Jallet, D., Shi, L., Rithner, C., Zhang, Y. & Peers, G. (2016). Quantification of chrysolaminarin from the model diatom *Phaeodactylum tricornerutum*. *Algal Research*, **20**: 180–188.
- Chiovitti, A., Higgins, M.J., Harper, R.E., Wetherbee, R. & Bacic, A. (2003a). The complex polysaccharides of the raphid diatom *Pinnularia viridis* (Bacillariophyceae). *Journal of Phycology*, **39**: 543–554.
- Chiovitti, A., Bacic, A., Burke, J. & Wetherbee, R. (2003b). Heterogeneous xylose-rich glycans are associated with extracellular glycoproteins from the biofouling diatom *Craspedostauros australis* (Bacillariophyceae). *European Journal of Phycology*, **38**: 351–360.
- Chiovitti, A., Molino, P., Crawford, S.A., Teng, R., Spurck, T. & Wetherbee, R. (2004). The glucans extracted with warm water from diatoms are mainly derived from intracellular chrysolaminaran and not extracellular polysaccharides. *European Journal of Phycology*, **39**: 117–128.
- Ciucanu, I. & Kerek, F. (1984). A simple and rapid method for the permethylation of carbohydrates. *Carbohydrate Research*, **131**: 209–217.
- Daglio, Y., Maidana, N.I., Matulewicz, M.C. & Rodríguez, M.C. (2016). Changes in motility and induction of enzymatic activity by nitrogen and phosphate deficiency in benthic *Halamphora luciae* (Bacillariophyceae) from Argentina. *Phycologia*, **55**: 493–505.
- Danielewicz, M.A., Anderson, L.A. & Franz, A.K. (2011). Triacylglycerol profiling of marine microalgae by mass spectrometry. *Journal of Lipid Research*, **52**: 2101–2118.
- De Bruyne, K., Slabbinck, B., Waegeman, W., Vauterin, P., De Baets, B. & Vandamme, P. (2011). Bacterial species identification from MALDI-TOF mass spectra through data analysis and machine learning. *Systematic and Applied Microbiology*, **34**: 20–29.
- Di Rienzo, J.A., Casanoves, F., Balzarini, M.G., González, L., Tablada, M. & Robledo, C.W. (2014). Grupo InfoStat, FCA, Universidad Nacional de Córdoba, Argentina. Available at: <http://www.infostat.com.ar>.
- Emami, K., Hack, E., Nelson, A., Brain, C.M., Lyne, F.M. & Mesbahi, E. (2015). Proteomic-based biotyping reveals hidden diversity within a microalgae culture collection: an example using *Dunaliella*. *Scientific Reports*, **5**: 2–15.
- Field, C.B., Behrenfeld, M.J., Randerson, J.T. & Falkowski, P. (1998). Primary production of the biosphere: integrating terrestrial and oceanic components. *Science*, **281**: 237–240.
- Giebel, R., Worden, C., Rust, S.M., Kleinheinz, G.T. & Robbins, M. (2010). Microbial fingerprinting using matrix-assisted laser desorption ionization time-of-flight mass spectrometry (MALDI-TOF MS): applications and challenges. *Advances in Applied Microbiology*, **71**: 149–184.
- Granum, E., Kirkvold, S. & Mykkestad, S.M. (2002). Cellular and extracellular production of carbohydrates and amino acids by the marine diatom *Skeletonema costatum*: diel variations and effects of N depletion. *Marine Ecology Progress Series*, **242**: 83–94.
- Gügi, B., Le Costaouec, T., Burel, C., Lerouge, P., Helbert, W. & Bardor, M. (2015). Diatom-specific oligosaccharide and polysaccharide structures help to unravel biosynthetic capabilities in diatoms. *Marine Drugs*, **13**: 5993–6018.
- Guillard, R.R.L. (1975). Culture of phytoplankton for feeding marine invertebrates. In *Culture of Marine Invertebrate Animals* (Smith, W.L. & Chanley, M.H., editors), 26–60. Plenum Press, New York, NY.
- Hildebrand, M., Manandhar-Shrestha, K. & Abbriano, R. (2017). Effects of chrysolaminarin synthase knockdown in the diatom *Thalassiosira pseudonana*: implications of reduced carbohydrate storage relative to green algae. *Algal Research*, **23**, 66–77.
- Hockin, N.L., Mock, T., Mulholland, F., Kopriva, S. & Malin, G. (2012). The response of diatom central carbon metabolism to nitrogen starvation is different from that of green algae and higher plants. *Plant Physiology*, **158**: 299–312.
- Jallet, D., Caballero, M.A., Gallina, A.A., Youngblood, M. & Peers, G. (2016). Photosynthetic physiology and biomass partitioning in the model diatom *Phaeodactylum tricornerutum* grown in a sinusoidal light regime. *Algal Research*, **18**: 51–60.
- Ju, Z., Ding, L., Zheng, Q., Wu, Z. & Zheng, F. (2011). Diatoms as a model system in studying lipid biosynthesis regulation. *International Journal of Environmental Science and Development*, **2**: 493–495.
- Kim, H.S., Hong, J.T., Kim, Y. & Han, S. (2011). Stimulatory effect of β -glucans on immune cells. *Immune Network*, **11**: 191–195.
- Knoshaug, E.P. & Darzins, A. (2011). Algal biofuels: the process. *Chemical Engineering Progress*, **107**: 37–47.
- Krishnamurthy, K.V. (1999). Fluorescence microscopic cytochemistry. In *Methods in Cell Wall Cytochemistry* (Krishnamurthy, K.V., editor), 151–176. CRC Press, Boca Raton, Florida.
- Le Costaouec, T., Unamunzaga, C., Mantecon, L. & Helbert, W. (2017). New structural insights into the cell-wall polysaccharide of the diatom *Phaeodactylum tricornerutum*. *Algal Research*, **26**: 172–179.
- Levitán, O., Dinamarca, J., Zelzion, E., Lun, D., Guerra, L. T., Kim, M.K., Kim, J., Van Mooy, B.A.S., Bhattacharyab, D. & Falkowski, P. (2015). Remodeling of intermediate metabolism in the diatom *Phaeodactylum tricornerutum* under nitrogen stress. *Proceedings of the National Academy of Sciences USA*, **112**: 412–417.
- Liang, J.R., Ai, X.X., Gao, Y.H. & Chen, C.P. (2013). MALDI-TOF MS analysis of the extracellular polysaccharides released by the diatom *Thalassiosira pseudonana*. *Journal of Applied Phycology*, **25**: 477–484.
- Martín, L.A., Popovich, C.A., Martínez, A.M., Damiani, M. C. & Leonardi, P.I. (2016). Oil assessment of *Halamphora coffeaeformis* diatom growing in a hybrid

- two-stage system for biodiesel production. *Renewable Energy*, **92**: 127–135.
- McConville, M.J., Bacic, A. & Clarke, A.E. (1986). Structural studies of chrysolaminaran from the ice diatom *Stauroneis amphioxys* (Gregory). *Carbohydrate Research*, **153**: 330–333.
- Myklestad, S. (1989). Production, chemical structure, metabolism, and biological function of the (1→3)-Linked, β 3-D-glucans in diatoms. *Biological Oceanography*, **6**: 313–326.
- Nelson, D.M., Tréguer, P., Brzezinski, M.A., Leynaert, A. & Quéguiner, B. (1995). Production and dissolution of biogenic silica in the ocean: revised global estimates, comparison with regional data and relationship to biogenic sedimentation. *Global Biogeochemical Cycles*, **9**: 359–372.
- Ng, W. (2013). Teaching microbial identification with matrix-assisted laser desorption/ionization time-of-flight mass spectrometry (MALDI-TOF MS) and bioinformatics tools. *Journal of Microbiology & Biology Education*, **14**: 103–106.
- Nicolau, A., Santos, L., Santos, C. & Mota, M. (2014). Matrix assisted laser desorption/ionisation time of flight mass spectrometry (MALDI-TOF-MS) applied to diatom identification: influence of culturing age. *Aquatic Biology*, **20**: 139–144.
- Nonami, H., Fukui, S. & Erra-Balsells, R. (1997). β -carboline alkaloids as matrices for matrix-assisted ultraviolet laser desorption time-of-flight mass spectrometry of proteins and sulfated oligosaccharides: a comparative study using phenylcarbonyl compounds, carbazoles and classical matrices. *Journal of Mass Spectrometry*, **32**: 287–296.
- Obata, T., Fernie, A.R. & Nunes-Nesi, A. (2013). The central carbon and energy metabolism of marine diatoms. *Metabolites*, **3**: 325–346.
- Packeu, A., Hendrickx, M., Beguin, H., Martiny, D., Vandenberg, O. & Detandt, M. (2013). Identification of the *Trichophyton mentagrophytes* complex species using MALDI-TOF mass spectrometry. *Medical Mycology*, **51**: 580–585.
- Paulsen, B.S. & Myklestad, S. (1978). Structural studies of the reserve glucan produced by the marine diatom *Skeletonema costatum* (Grev.) Cleve. *Carbohydrate Research*, **62**: 386–388.
- Pavlovic, M., Mewes, A., Maggipinto, M., Schmidt, W., Messelhauser, U. & Balsliemke, J. (2014). MALDI-TOF-MS based identification of food-borne yeast isolates. *Journal of Microbiological Methods*, **106**: 123–128.
- Sandrin, T.R., Goldstein, J.E. & Schumaker, S. (2013). MALDI-TOF MS profiling of bacteria at the strain level: a review. *Mass Spectrometry Review*, **32**: 188–217.
- Shea, E.M. & Carpita, N.C. (1988). Separation of partially methylated alditol acetates on SP-2330 and HP-1 vitreous silica capillary columns. *Journal of Chromatography*, **445**: 424–428.
- Smith, V.H. & Crews, T. (2014). Applying ecological principles of crop cultivation in large-scale algal biomass production. *Algal Research*, **4**: 23–34.
- Stone, B. (2006). Callose and related glucans. *Encyclopedia of Life Sciences*. doi: 10.1038/npg.els.00041.
- Storseth, T.R., Kirkvold, S., Skjermo, J. & Reitan, K. (2006). A branched β -D-(1→3, 1→6)-glucan from the marine diatom *Chaetoceros debilis* (Bacillariophyceae) characterized by NMR. *Carbohydrate Research*, **341**: 2108–2114.
- Sumper, M. & Lehmann, G. (2006). Silica pattern formation in diatoms: species-specific polyamine biosynthesis. *ChemBioChem*, **7**: 1419–1427.
- Sumper, M., Brunner, E. & Lehmann, G. (2005). Biomineralization in diatoms: characterization of novel polyamines associated with silica. *FEBS Letters*, **579**: 3765–3769.
- Sumper, M., Hett, R., Lehmann, G. & Wenzl, S. (2007). A code for lysine modifications of a silica biomineralizing silaffin protein. *Angewandte Chemie*, **46**: 8405–8408.
- Suzuki, T., Midonoya, H. & Shioi, Y. (2009). Analysis of chlorophylls and their derivatives by matrix-assisted laser desorption/ionization-time-of-flight mass spectrometry. *Analytical Biochemistry*, **390**: 57–62.
- Takahashi, E., Ledauphin, J., Goux, D. & Orvain, F. (2009). Optimising extraction of extracellular polymeric substances (EPS) from benthic diatoms: comparison of the efficiency of six EPS extraction methods. *Marine and Freshwater Research*, **60**: 1201–1210.
- Tesson, B. & Hildebrand, M. (2013). Characterization and localization of insoluble organic matrices associated with diatom cell walls: insight into their roles during cell wall formation. *PLoS ONE* **8**(4): e61675.
- Tréguer, P., Bowler, C., Moriceau, B., Dutkiewicz, S., Gehlen, M., Aumont, O., Bittner, L., Dugdale, R., Finkel, Z., Iudicone, D., Jahn, O., Guidi, L., Lasbleiz, M., Leblanc, K., Levy, M. & Pondaven, P. (2017). Influence of diatom diversity on the ocean biological carbon pump. *Nature Geoscience*, **11**: 27–37.
- Vieler, A., Wilhelm, C., Goss, R., Süß, R. & Schiller, J. (2007). The lipid composition of the unicellular green alga *Chlamydomonas reinhardtii* and the diatom *Cyclotella meneghiniana* investigated by MALDI-TOF MS and TLC. *Chemistry and Physics of Lipids*, **150**: 143–155.
- Waterkeyn, L. & Bienfait, A. (1987). Localization and function of beta 1,3-glucans (callose and chrysolaminarin) in *Pinnularia* genus (Diatoms). *Cellule*, **74**: 199–226.
- Wilhelm, C., Büchel, C., Fisahn, J., Goss, R., Jakob, T., Laroche, J., Lavaud, J., Lohr, M., Riebesell, U., Stehfest, K., Valentin, K. & Kroth, P.G. (2006). The regulation of carbon and nutrient assimilation in diatoms is significantly different from green algae. *Protist*, **157**: 91–124.
- Xia, S., Gao, B., Li, A., Xiong, J., Ao, Z. & Zhang, C. (2014). Preliminary characterization, antioxidant properties and production of chrysolaminarin from marine diatom *Odontella aurita*. *Marine Drugs*, **12**: 4883–4897.
- Young, R.J. & Lovell, P.A. (1991). *Introduction to Polymers*, 2nd edition. Cambridge University Press, Cambridge.
- Zhang, H., Wang, D.Z., Xie, Z.X., Zhang, S.F., Wang, M.H. & Lin, L. (2015). Comparative proteomics reveals highly and differentially expressed proteins in field-collected and laboratory-cultured blooming cells of the diatom *Skeletonema costatum*. *Environmental Microbiology*, **17**: 3976–3991.